Quantitative imaging of collective cell migration during *Drosophila* gastrulation: multiphoton microscopy and computational analysis

Willy Supatto[1,2], **Amy McMahon**, **Scott E. Fraser**, and **Angelike Stathopoulos**[1]
California Institute of Technology Beckman Institute and Division of Biology Pasadena, CA USA

Abstract

This protocol describes imaging and computational tools to collect and analyze live imaging data of embryonic cell migration. Our five step protocol requires a few weeks to move through embryo preparation and four-dimensional (4D) live imaging using multiphoton microscopy, to 3D cell-tracking using image processing, registration of tracking data, and their quantitative analysis using computational tools. It uses commercially available equipment, and requires expertise in microscopy and programming that is appropriate for a biology laboratory. Custom-made scripts are provided, as well as sample datasets to permit readers without experimental data to perform the analysis. The protocol has offered new insights into the genetic control of cell migration during *Drosophila* gastrulation. With simple changes, this systematic analysis could be applied to any developing system to define cell positions in accordance with the body plan, to decompose complex 3D movements, and to quantify the collective nature of cell migration.

INTRODUCTION

Quantitative imaging of collective cell migration in a developing embryo

The combination of advanced imaging and image analysis techniques enables the investigation of large, dynamic cell populations within a developing embryo[1,2]. These imaging approaches provide a unique opportunity to study embryonic morphogenesis from the level of cellular processes to the scale of an entire tissue or organism. Gastrulation in the *Drosophila melanogaster* embryo is an excellent model system for the study of embryonic morphogenesis[3]. In less than two hours of development, ~6000 cells undergo stereotypical morphogenetic events, such as tissue invagination[4], convergence-extension[5,6], planar cell intercalation[5,6], radial cell intercalation[1], epithelial-to-mesenchymal transition[7], synchronized waves of cell division[1], and collective cell migration[1]. Although the geometry of the *Drosophila* embryo is relatively simple at early stages of development, the morphogenetic events involve highly dynamic processes and complex 3D movements of cells that prevent a complete investigation of most wild-type or mutant phenotypes based on the analysis of fixed embryos.

This protocol presents the quantitative imaging of complex cell migration *in vivo*, using mesoderm cell spreading during *Drosophila* gastrulation as a model system. The experimental

strategy combines 4D *in vivo* imaging using 2-photon excited fluorescence (2PEF) microscopy, 3D-cell tracking using image processing, and automated analysis of cell trajectories using computational tools. This quantitative approach decomposes 3D cell movements, generating a precise description of morphogenetic events. Furthermore, this protocol describes the quantitative investigation of the collective nature of mesoderm cell migration. The reproducibility of morphogenetic events among wild-type embryos can be tested and mutant phenotypes can be dynamically analyzed. This approach provides a method to study complex or even subtle mutant phenotypes, such as the ability to distinguish cell populations that exhibit different behaviors[1]. We recently applied this approach to gain insights into the control of cell migration during mesoderm formation in *Drosophila* embryos[1].

Experimental Design

The experimental workflow is divided into five main parts (Fig. 1): the embryo preparation (steps 1–9), the 4D-imaging (steps 10–15), the 3D-cell tracking (steps 16–22), the tracking data registration (steps 23–27), and the tracking data analysis (step 28). Flies containing a fluorescent reporter are mated and embryos are collected. The chorion is removed and the embryos are mounted for live imaging and 4D image dataset acquisition using a 2PEF microscope. Typically ~2,000 mesoderm and ectoderm cells moving through the field of view are imaged during 2–3 hours of development. Each imaging dataset contains ~10^9 voxels and is processed using Imaris software to track the trajectories of the cell collection. Finally, a quantitative and automated analysis of the cell trajectories is performed using Matlab. Customized Matlab scripts required to perform steps 23–28 are provided in the supplemental section of this protocol (**Supplementary Data 1**). A sample dataset is also provided to allow readers to start the procedure at step 23 without having to collect experimental data (**Supplementary Data 2**). This protocol can be directly applied to study mesoderm spreading in gastrulating *Drosophila* embryos. However, the workflow is not specific to this particular stage or model system. In addition, each part described in Fig. 1 can be used independently and included into a different working strategy. In order to facilitate the adaptation of this protocol to other stages or model organisms, we discuss below each part of the workflow with general comments and advice that are summarized in Table 1. The specific experimental choices made to study *Drosophila* gastrulation are clearly indicated.

Embryo preparation

Nuclear fluorescent labeling—A critical component of this protocol is the choice of the fluorescent reporter, as this reporter must be suitable both for high quality imaging and cell movement quantification. To this end, fluorescent labeling of nuclei provides several advantages: (i) the nuclei are easier to segment and track from 4D image datasets than other cellular structures, such as membranes; (ii) the spatial position of the segmented nucleus can directly define the spatial position of a cell for cell movement analysis; (iii) nuclear fluorescent labeling provides a direct indicator of cell division; and (iv) transgenic lines *of Drosophila* with a strong, stable, and ubiquitous expression of fluorescent protein fused with histone or nuclear localization sequence are available (see Reagents section and Bloomington Stock Center, for instance). The lines expressing in-frame fusions of GFP to a nuclear localization sequence (NLS) have the disadvantage of producing a diffuse fluorescent signal each time the nuclear envelope breaks down during each cell division (Supplementary Movie 1). In this protocol, we used the transgenic line expressing GFP fused with Histone 2A available from Bloomington Stock Center (see Reagents section). The fluorescent Histone remains associated with the chromosomes even during nuclear envelope breakdown, giving an unambiguous signal for tracking[1].

Sample optical properties and *klarsicht* mutant—The scattering of light inside the biological sample is usually the factor limiting the depth of imaging. The scattering property

of the embryonic tissue is developmental stage- and species-dependant (**Box 1** and Fig. 2). During *Drosophila* gastrulation, a high density of sub-micrometer scale refractive vesicles, mostly lipid droplets, are observed in cells and at the surface of the yolk[8]. These lipid bodies are strong light scatterers, which results in the high scattering property of early embryos and prevents deep tissue imaging. The distribution of these lipid bodies is altered in *klarsicht (klar)* mutants: the lack of Klar in these embryos prevents the apical redistribution of lipid bodies at the end of cellularization, yet the homozygous mutants are viable[9]. As a result, *klar* cells appear more transparent than wild-type during gastrulation (Fig. 2a–b). We compared the optical properties of wild-type and *klar* embryos at stage 8 (stages defined by[10]) by measuring the scattering mean free path, l^{ex}_s, of the near-infrared (NIR) light (**Box 1** and Fig. 2c). l^{ex}_s is ~56μm in wild-type embryos (blue in Fig. 2d) and ~76μm in *klar* embryos (red in Fig. 2d). From these measurements, the typical 2PEF signal decay depending on the depth of imaging can be plotted (Fig. 2e, see details in **Box 1**). It shows that the higher value of l^{ex}_s in *klar* compared to wild-type embryos is sufficient to double the intensity of 2PEF signal recorded at 80 μm depth (compare blue and red curves in Fig. 2e). In this protocol, we used the *klar* background to improve the imaging depth and the level of signal - two criteria that significantly facilitate image processing. Of note is the fact that we did not observe any disruption of mesoderm migration in *klar* embryos[1], therefore conducting experiments in a *klar* mutant background provides a good option to improve imaging capabilities.

To show the scattering properties of embryonic tissues and the subsequent limitation of imaging depth are stage- and species-dependant, we plotted the depth-dependent 2PEF signal from stage 5 *Drosophila* or early *zebrafish* mesoderm (gray curves in Fig. 2e) based on the previous experimental measurement of the scattering properties (gray in Fig. 2d). The signal decay demonstrates that stage 5 and stage 8 *Drosophila* embryos (dark gray and blue curves in Fig. 2e, respectively) exhibit significantly different properties, whereas these two stages are separated by only 1 hour of development. In addition, the 2PEF signal at 80 μm is expected to be 5 times weaker in *Drosophila* at gastrulation (blue curve in Fig. 2e) compared to early *zebrafish* embryos (light gray in Fig. 2e) for the same labeling and imaging conditions. Hence, the maximum depth of imaging and the choice of the microscopy technique depend on the stage and model system. For instance, as opposed to *Drosophila* embryos, the imaging of mesoderm structures at 80 μm in early zebrafish embryos is achievable with confocal microscopy and does not require 2PEF microscopy[11].

Embryo mounting procedure—The mounting procedure is a critical step of the embryo preparation for optimized imaging. The use of materials inducing optical aberrations on the optical path, such as agarose gel, should be avoided or limited. In order to enable a proper quantification of cell movements and avoid motion artifacts, the embryos must be precisely oriented and maintained in place during the image acquisition. Furthermore, the mounting of the embryos should not deform the embryo itself (for instance, by squeezing the embryo between coverslips), as this might alter the cell behaviors. In the case of *Drosophila* embryos, we found that mounting them in water and imaging without an additional coverslip between the specimen and the objective offered the best compromise between embryo health and image quality. This arrangement avoids the refractive index mismatch between embryo and immersion solution that would be present with an oil-immersion objective, prevents embryo hypoxia, and does not induce deformation. The embryos are oriented and maintained in place by gluing them on a coverslip. The orientation is first based on the shape of the embryo: the dorsal side has less curvature than the ventral side (Supplemental Movie 2). The well-oriented embryos are then selected at early stage 6 under the 2PEF microscope[10] with the ventral side facing the objective. The onset of ventral furrow formation at stage 6 makes it easy to identify well-oriented embryos: the furrow should face the objective, in the middle of the field of view.

4D-imaging

Multiphoton microscopy for *in vivo* imaging of scattering embryos—Choosing the appropriate microscopy technique to image living embryos depends on several criteria: the required spatial and temporal resolution, the size or shape of the embryo and volume to image, the sensitivity to phototoxicity, and the optical properties of the tissue. Imaging the early stages of *Drosophila* gastrulation is limited by two major factors: the light scattering properties of the tissue and the phototoxicity. These limitations are especially apparent when imaging mesoderm formation using confocal microscopy. When using confocal microscopy only half of the required depth is visualized and the required spatio-temporal sampling quickly induces strong phototoxicity (see below). 2PEF microscopy[12] and other multiphoton microscopy techniques[8], are better choices to support the 4D (3D in space and 1D in time), long-term, deep-tissue imaging of *Drosophila* embryos in a manner that does not compromise their viability.

In multiphoton microscopy, the sample is illuminated with NIR radiation and the spatial resolution is intrinsically three-dimensional, resulting in: (i) good penetration and low absorption of the excitation light, and (ii) efficient collection of the emitted light, including scattered photons, due to the absence of pinhole. We reported the imaging of internalized mesoderm cells up to a depth of 80μm within the embryo using 2PEF[1]. Another significant advantage of using NIR radiation, compared to the linear excitation at 488 nm used in standard fluorescence microscopy, is that the nonlinear excitation of GFP can be obtained using a wavelength (see below) inducing a lower background (i.e., auto-fluorescence).

The main limitation of 2PEF microscopy, as with any laser scanning microscopy, is the time of acquisition. Although *Drosophila* embryonic development is fast, the morphogenetic movements are slow enough to be captured with laser scanning microscopy. However, the acquisition speed becomes a limitation when imaging a large volume of cells while trying to maintain good spatial and temporal sampling. As a consequence and in order to avoid phototoxicity and obtain a signal level and spatio-temporal sampling suitable for proper image analysis, the 2PEF imaging of *Drosophila* mesoderm cells requires careful adjustment of the imaging parameters (i.e., objective, spatial and temporal sampling, field of view, resting time, laser power, wavelength).

Phototoxicity—The depth of imaging, the level of fluorescent signal, and the speed of acquisition required for this procedure can easily lead the investigator to use imaging conditions that induce phototoxic effects and prevent the normal development of the imaged embryo. For this reason, it is important to systematically check for any sign of photo-induced effects on movement. The imaging parameters must be carefully tuned in order to stay far away from phototoxic conditions while maintaining sufficient image quality to support the subsequent image processing steps. Though the molecular mechanisms resulting in phototoxicity in 2PEF microscopy are not fully understood, phototoxic processes usually appear to be highly nonlinear[13, 14]: meaning that the threshold is sharp and that small changes in imaging parameters are enough to switch from toxic to non-toxic conditions.

Several criteria can be used to identify phototoxic effects in *Drosophila* during gastrulation. The level of endogenous fluorescent signal (also called autofluorescence) is often a good indicator. If the endogenous signal from the yolk or the vitelline membrane begins to approach the level of the GFP fluorescent signal, it indicates that the imaging conditions will most likely induce phototoxicity. In this case, a different GFP labeling and/or a different excitation wavelength should be used. The cell movements can indicate phototoxicity: if these movements slow down independently of the temperature and specifically within the field of view, it is a clear effect of phototoxicity. Finally, it is possible to observe more subtle effects at low laser power level, including changes affecting cell division rates. Cell divisions occurring a few

minutes earlier or later than normal induce a disruption of the cell division pattern that can be quantified[1]. We interpret this effect as a mild disruption of cytoskeleton dynamics. Lastly, it is important to note that phototoxic effects may result long before any photo-bleaching is induced. Hence, the mere absence of photobleaching is not a good indicator of non-invasiveness.

How to choose the appropriate objective—For the deep-tissue imaging of highly scattering tissue using 2PEF microscopy, the ideal objective must have a large working distance, a high numerical aperture (NA), a low magnification, and good transmission of NIR light. The large working distance prevents embryo hypoxia and allows deep-tissue imaging. The high NA improves the spatial resolution, the 2-photon excitation, and the light collection efficiency. The low magnification allows image acquisition from a large area, which significantly improves 2PEF signal collection efficiency[15]. For this procedure, we used a 40x water immersion objective with 1.1 NA and working distance of 600μm.

How to choose the appropriate excitation wavelength—The choice of the excitation wavelength is critical to obtain an efficient fluorophore excitation, a low endogeneous signal (background), and low phototoxicity. Use of a tunable femtosecond laser allows the user to test different wavelengths and choose the best compromise. When imaging GFP, the optimal 2-photon excitation wavelength is 940–950nm. We observed that in gastrulating *Drosophila* embryos, the use of lower wavelengths leads to higher phototoxicity, lower GFP excitation efficiency, as well as higher levels of endogenous fluorescent signal. Consequently, in this case, the absorption of water in the 950nm wavelength range does not play a significant role in the phototoxicity.

Improved collection efficiency of scattered photons in 2PEF microscopy—In most techniques of fluorescence microscopy, such as confocal microscopy, only the ballistic photons that are not scattered from the emission spot en route to the detector contribute to the fluorescent signal. As the fluorescence excitation is restricted to the focal volume in 2PEF microscopy, every emitted photons can contribute to the signal, including scattered photons. In practice, it means that the signal collected from scattering tissue can be improved by collecting light in every spatial direction. For instance, the 2PEF signal can be collected in both the trans- and epi-direction if the microscope setup permits it. In our case, we added a silver mirror in the trans-direction, which reflects forward-directed photons and contributes to collection of some of them by the objective in the epi-direction. This straightforward procedure allowed us to collect up to 30% more 2PEF signal with the same illumination conditions, thus significantly improving the image quality and facilitating the image processing steps.

How to choose the appropriate spatial and time sampling—The spatial resolution has to be sufficient for the proper segmentation of nuclei. Even if the tracked objects are large (nuclei are of ~5–10 μm diameter), the gap between them can be small (< 2 μm). As a result, a high NA objective is required, especially for the segmentation of nuclei located deep within the embryo. A spatial sampling of 0.5 μm per pixel in x,y direction and 1 μm in z appears sufficient.

The time resolution is critical in order to ensure error-free cell tracking, and to avoid the incorrect assignment of cell identities due to temporal aliasing. Temporal aliasing occurs when 3D stacks of images are acquired with a time interval between two frames too large to permit faithful cell tracking. Indistinguishable nuclei travel with a velocity v and are separated by a distance d. When images are acquired with a time interval Δt between two stacks, for the nuclear trajectory to be extracted unambiguously the distance $v.\Delta t$ travelled by the cell in between two stacks must be less than half the distance d (i.e., $v.\Delta t < d/2$)[16]. In our case, as v~5μm.min^{-1} and d~10μm, thus the requirement is that $\Delta t < 1$ min. We used $\Delta t = 45$–50 seconds.

3D-Cell Tracking

Image processing techniques other than cell tracking have been successfully applied to quantify morphogenetic movements in embryos. For instance, image cross-correlation velocimetry[12, 17,18] isspecifically adapted to measure tissue deformation by direct differential analysis of the estimated velocity field[12]. However, the spatial resolution is limited by the size of the image interrogation window and this approach is usually limited to 2D. Cell tracking based on the segmentation and tracking of nuclei provides an opportunity to follow the behavior of individual cells in 3D with good spatial and temporal resolution (Fig. 3).

The quality of the image dataset is critical for the proper tracking of cell movements; any slight improvement of this dataset can drastically improve the image processing. For instance, as discussed above, the signal level as well as the spatial and temporal resolution is critical for proper nuclear segmentation and tracking (Table 1).

We choose to use Imaris software to perform 3D-cell tracking for several reasons. First, the user interface and the 3D visualization of the imaging dataset are extremely efficient. The cell tracks can be visualized, checked and manually corrected using the tracking editor (provided in version 5.7). The Imaris XT interface with Matlab improves the functionality of the software without extensive knowledge of computer programming: for instance, the data can be exported into Matlab for further analysis. Together, it appears to be a good compromise option, as it combines the user-friendly interface and standard analysis of commercial software with sufficient flexibility that the user can customize the tools for their applications without the need to write a completely custom software package. Because an improved background knowledge of Imaris software and its functionalities can drastically reduce the time spent performing 3D-cell tracking of a large dataset, users should consider obtaining experience with the software from Bitplane through user-training sessions (contact Bitplane customer service for details).

This protocol describes the tracking of two cell populations during *Drosophila* gastrulation: mesoderm and ectoderm cells. These two groups are defined by sorting the cell trajectories using Imaris functions. The mesoderm cells are those that have invaginated and the ectoderm cells stay at the surface of the embryo. A few midline cells (a sub-population of the ectoderm) are independently tracked and their trajectories are used for spatial registration (see below). The tracking of mesoderm and midline cells is carefully checked so that the trajectories span the entire time sequence.

Tracking Data Registration

The registration is an important step including any spatial or temporal transformation of the datasets that enables their comparison from one experiment to the other. This protocol describes three types of data registration: the correction of motion artifacts, the transformation of the adapted spatial coordinate system, and the synchronization of imaging sequences (Table 1 and Fig. 4–5).

In image analysis, different methods of registration exist. For instance, the distribution of specific markers in the sample can be used to correct its drift during time of acquisition (landmark-based spatial registration), or the voxel values of an image sequence can be used to synchronize several datasets (voxel-based temporal registration19). In this procedure, we used the segmented objects themselves to perform both spatial and temporal registration in a fully quantitative and automated manner. For this reason, the registration is performed after the 3D-cell tracking. Under some experimental conditions, spatial registration has to be done before 3D-cell tracking; for instance, strong motion artifacts during the image acquisition (embryo rolling, sample or stage drift, etc) can degrade the cell tracking process.

In this protocol, the spatial registration includes the definition of cell positions in accordance with the body plan. The choice of a spatial coordinate system adapted to the geometry of the tissue or embryo enable the user to investigate complex cell movements in 3D by decomposing their trajectories into components that have a biological meaning. The appropriate coordinate system depends on the biological model used: for instance, during early stages of development, a spherical coordinate system is adapted to the shape of zebrafish[2] or *Xenopus Laevis*[20], whereas a Cartesian coordinate system remains appropriate for avian embryos[18]. In the case of *Drosophila* gastrulation, the embryo has a cylindrical shape in the area where mesoderm spreading occurs (Supplemental Movie 2). The protocol shows first how a cylinder is fitted onto the spatial distribution of ectoderm cells (EctodermCylinderFit.m Matlab script, **Supplemental Data 1** and Table 2) in order to identify the anterior-posterior axis of the embryo and to switch from Cartesian (x, y, z) to cylindrical (r, θ, z) coordinate system (Fig. 4). In this coordinate system, the movements in each direction (radial, angular or longitudinal) can be directly compared from one embryo to the other and correspond to specific morphogenetic events[1].

The final step of spatial registration is the angular drift correction (Registration.m Matlab script, **Supplemental Data 1** and Table 2). During the time of acquisition, the embryo can exhibit some rolling inside its vitelline membrane, corresponding to a solid rotation around the anterior-posterior axis (Supplemental Movies 2–3). This angular drift is corrected by tracking a few cells from the ectoderm midline and defining their angular position at each time point as θ=0 radian (Fig. 5a–c).

The temporal registration corresponds to the synchronization of image sequences based on the occurrence of a specific morphogenetic event (TimeSynchronization.m Matlab script, **Supplemental Data 1** and Table 2). We choose the onset of germband extension (GBE)[5, 6] as the time reference to synchronize the sequences and define t=0 min (Fig. 5d). At this time, both ectoderm and mesoderm cells start to move toward the posterior direction[1].

It is important to notice that the references used for spatial and temporal registration are identical among embryos and are not disrupted in mutants. Hence, they depend on the model system studied. In this protocol, the estimation of the anterior-posterior axis using the shape of the ectoderm layer, the angular reference θ=0 rad using the ectoderm midline cells and the time synchronization based on the onset of GBE are independent of the mesoderm spreading process. In addition, we used these references for registration because they are not disrupted in the mutant we studied[1].

Tracking Data Analysis

Once the tracking data are registered, the cell trajectories can be analyzed directly and compared from one embryo to the other. We provide two examples of tracking data analysis useful for studying complex 3D movements of cell migration and quantifying the collective nature of this process: decomposition of cell trajectories along each cylindrical direction (Fig. 6) using MovementDecomp.m Matlab script (**Supplemental Data 1** and Table 2) and mesoderm spreading analysis (Fig. 7) using SpreadingAnalysis.m Matlab script (**Supplemental Data 1** and Table 2).

Advantages and limitations of this protocol to investigate *in vivo* cell migration

There are number of protocols available to investigate cell migration in tissue culture or in model organisms (see[21] for instance). Here we discuss the advantages and specificity of this protocol for studying cell migration *in vivo*:

(i) The cells are imaged in challenging conditions: they move fast and deep inside a scattering and photo-sensitive embryo. Hence, we describe here an optimized imaging approach.

(ii) Most studies of cell migration are limited to 2D in space and to cells migrating on a fixed substrate; however, inside a living organism, it usually occurs in 3D, with the simultaneous combination of different movements. This protocol shows how to investigate such complex movements in 3D by choosing the appropriate spatial coordinate system and decomposing the cell trajectories into meaningful components. In this study, the mesoderm cells migrate on a moving cell layer (ectoderm): we recently demonstrated how the data generated by this protocol allowed us to investigate the mechanical coupling between two cell layers and to decouple their movements[1].

(iii) During embryonic development, cells rarely migrate alone but more often as a collective. The method for tracking a large cell population described in this protocol allows for simultaneous observation of individual and collective behaviors, both of migrating and non-migrating cells. This approach allows the investigator to evaluate migration with a statistical analysis and to identify variability within the cell population[1]. By following a limited number of cells using techniques such as local photo-activation, one can focus on specific behaviors, but they may not necessarily be representative of the collective.

(iv) Whereas many studies analyze the cell tracking results using a qualitative or manual approach, we provide a quantitative and automated analysis of cell trajectories. In this protocol, the spatial and temporal registration of the data enables the investigator to quantitatively compare one experiment to the other, to test the reproducibility between embryos and to quantify mutant phenotypes[1]. In addition, the statistical analysis of cell trajectories presented here illustrates how to quantify the collective nature of a cell migration process.

(v) Sophisticated quantitative imaging of cell movements usually involves fully custom-designed approaches that are difficult to implement or modify by other laboratories without strong expertise[2]. This protocol uses commercially available equipment and software and provides customized Matlab scripts that are annotated and simple enough to be used and modified with minimal expertise. Imaris, the commercial software used to perform 3D-cell tracking is extremely user-friendly; its interface ImarisXT, can be used with classic programming languages and image processing software, such as Matlab or ImageJ, enabling a user with minimum skills in programming to improve the functionality of this software for specific scientific applications. Together, these aspects enable the user to implement, modify, or extend this protocol in a biology laboratory without extensive expertise in microscopy or computer science.

This protocol has two main limitations. First, cell migration is investigated by only tracking the cell nuclei. Although this approach can already generate a lot of biological insights, the analysis of other cell features, such as cell shape changes can be required for specific studies. In the case of mesoderm spreading in *Drosophila*, the challenging scattering conditions (see above) strongly limit the imaging of structures other than nuclei, such as cell membranes. The second limitation concerns the 3D-cell tracking: the fluorescent signal from the deepest nuclei is weak and their segmentation and tracking requires manual correction. This step, which is not fully automated, limits the number of cells segmented per experiment. For this reason, we limited our application of this protocol to ~100,000 segmented cell positions per embryo (including ectoderm and mesoderm cells)[1]. To increase this number, further improvement of imaging quality and/or of image segmentation/tracking strategy would be required. The subsequent computer analysis of cell trajectories provided here is automated and is not limited by the cell number.

MATERIALS

REAGENTS

- *Drosophila* transgenic line with an ubiquitous expression of Histone 2A-GFP fusion protein (Bloomington Drosophila Stock Center, stock number 5941) and *klarsicht* mutant line from Bloomington Drosophila Stock Center, stock number 3256)

- Halocarbon Oil 27 (Sigma, cat. no. H8773)

- Heptane (EMD, cat. no. HX0080)

- 50% (v/v) Bleach (Clorox) or Sodium hypochlorite (Reagent grade, Sigma, cat. no. 239305) **! Caution** Bleach is poisonous. Wear personal protection, such as gloves and goggles.

- Glacial acetic acid (VWR, cat. no. MK312146) **! Caution** Acetic acid is corrosive. Handle with gloves.

- Ethanol (Sigma-Aldrich, cat. no. 459836) **! Caution** Ethanol is flammable.

- UltraPure Agarose (Invitrogen, cat. no. 15510-019)

- Apple juice (generic brand)

- Sucrose (generic brand)

EQUIPMENT

- Paintbrush (small brush size: 3/0 White Sable Robert Simmons)

- Double-sided sticky tape (TESA) ▲ **CRITICAL** if another brand is used, ensure the glue is not toxic for the embryos.

- Coverslips (22×22mm, No1, VWR, cat. no. 48366 067)

- 35×10mm petri dishes (BD Falcon, cat. no. 353001)

- 60×15mm petri dishes (BD Falcon, cat. no. 353002)

- 2PEF Microscope: Zeiss LSM 510 with Chameleon Ultra Laser (Coherent Inc)

- C-Aprochromat 40×/1.1 N.A. W Corr UV-VIS-IR (Carl Zeiss Inc) objective.

- Software: Imaris 5.7 with ImarisTrack, Imaris MeasurementPro, and ImarisXT modules (Bitplane) and Matlab 7.7 (The MathWorks).

- Computer: 3.0 GHz Dual-Core Processor, 16 Gb DDR RAM, Large SATA Hard Drive (> 100 Gb, faster than 7000 rpm)

- 1 L glass bottles and 25 ml plastic pipettes.

- Optional: Thumbtack/Needle

- Small basket to handle the embryos. One can use: 100 μm - cell strainers (BD Falcon, cat. no. 352360)

- Standard dissecting microscope

REAGENT SETUP

Apple juice plate—Dissolve 22 g of sucrose in 350 ml of H_2O and pour it into a 1 L bottle. Add 7 g of agarose into this bottle, mix by vigorous shaking. Microwave first for 2 min, and then 2 times for 1 min, mixing the solution in between.

▲ CRITICAL the agarose solution must boil in the microwave.

Put aside to cool to approximately 60 °C. Add 10 ml of ethanol and 5 ml of glacial acetic acid to the solution. Add 50 ml of apple juice and mix well. Pipette into 35×10 mm dishes (~60 plates/preparation) using 25 ml plastic pipette or syringe. The plates can be stored in a container at 4°C for weeks.

! Caution Acetic acid is corrosive. Handle with gloves.

! Caution Ethanol is flammable.

Agarose plate—Dissolve 30 g of sucrose in 350 ml of H_2O and pour it into a 1 L bottle. Add 10 g of agarose to the bottle, mix by vigorous shaking. Microwave first for 2 min, and then 2 times for 1 min, mixing the solution in between.

▲ **CRITICAL** the agarose solution must boil in the microwave.

Put aside to cool to ~60 °C. Pipette into 60×15 mm dishes (~20 plates/preparation) using a 25 ml plastic pipette or syringe. The plates can be stored in a container at 4°C for weeks.

EQUIPMENT SETUP

Preparation of coverslips coated with glue for embryo imaging—Add short pieces (5–10 cm) of double-sided tape to a 200 ml glass bottle. Add heptane to cover the pieces of tape (typically 50 ml for 50 cm of tape). Gently shake the bottle at least overnight at room temperature (18–25 °C) to dissolve the glue. The heptane-glue bottle can be stored at room temperature for months. Prepare coverslips coated with glue at least 10 min before using them. Add a 60–100 μl droplet of heptane-glue to the middle of each coverslip and allow to dry for 10 min. The coated coverslips can be stored for a few days at room temperature in a box to protect them from dust.

Microscope settings for live imaging (Zeiss LSM 510)—Most of our imaging datasets have been acquired using a Zeiss LSM 510 microscope and a Chameleon Ultra femtosecond laser. However, the protocol can be accomplished with any similar 2PEF microscope. The embryos were imaged using C-Aprochromat 40×/1.1 N.A. W Corr UV-VIS-IR (Carl Zeiss Inc) objective at 940 nm. The non-descanned pathway is used with a single short pass filter (KP680nm) to cut out the laser light. $200 \times 200 \times 80 \mu m^3$ 3D-stacks with $0.5 \times 0.5 \times 1 \mu m^3$ voxel size and 1.9μs pixel dwell time were acquired every 45–50 seconds for ~3 h.

LSGE and geom3D toolboxes for Matlab processing—The Matlab processing requires two freely available toolboxes: the Least Squares Geometric Elements (LSGE) library and the geom3d toolbox. The LSGE library was developed by the Centre for Mathematics and Scientific Computing (National Physical Laboratory, UK) and is available from the EUROMETROS website (http://www.eurometros.org/gen_report.php?category=distributions&pkey=14). The geom3d toolbox was developed by David Legland and is available from Matlab Central website (http://www.mathworks.com/matlabcentral/fileexchange/8002). Download the files, save the "lsge-matlab" and "geom3D" folders and their content on you computer and add both of them in the Matlab path (using "File/Set Path" from the Matlab menu).

Customized Matlab scripts—Download the Matlab scripts from the supplemental section of this protocol (**Supplementary Data 1**). Unzip the corresponding file and place all contained files (Imaris2xyzt.m, EctodermCylinderFit.m, TimeSynchronization.m, Registration.m, MovementDecomp.m, SpreadingAnalysis.m, Browse.m, and cart2cyl0.m) in the same folder.

The customized Matlab scripts included here are designed and annotated in order to allow the user to run and modify them with only basic knowledge of Matlab programming. However, to further manipulate the data, a working knowledge of Matlab is required. Table 2 provides a list of the scripts and their description.

Sample tracking data files—In order to run the Matlab processing and start the procedure at step 23 without an imaging dataset, we provide sample tracking data files. Download the files from the supplemental section of this protocol (**Supplementary Data 2**). Unzip the corresponding file and place all of the files (Mesoderm.mat, Ectoderm.mat and Midline.mat) in the same folder as the Matlab scripts.

PROCEDURE

Embryo Preparation ● TIMING 4 h per set of embryos for imaging

1| Grow flies in standard culture bottles (the generation time is ~10 days at 25°C; see http://flystocks.bio.indiana.edu/Fly_Work/culturing.htm for details).

2| Transfer the flies into a collection bottle and add an apple juice plate (see Reagent Setup and standard procedure in22).

3| Collect the embryos after 2–3 h of laying at 25 °C.

4| Add a few droplets of halocarbon oil on the embryos to make the chorion translucent, stage the embryos[10], and select ~10–20 stage 5 embryos. Embryos reach stage 5 after 2–3 h of development. This stage is easily identified by looking at the transparent layer of cellularizing cells at the embryo periphery (see http://flymove.uni-muenster.de/ for pictures of stages).

5| Dechorionate the embryos using either option A Dechorionation with bleach or option B Dechorionation with a needle, depending on the user preference and ability.

    (A) Dechorionation with bleach

        (i) Transfer the embryos into a basket with a paintbrush.

        (ii) Remove the oil from the bottom with a paper towel.

        (iii) Rinse the embryos with a few ml of water.

        (iv) Soak the basket in fresh 50% bleach (vol/vol) and control the dechorionation by looking at the embryos under a dissecting microscope. When the first bubble appears between the chorion and the vitelline membrane of any embryo, immediately proceed to step v (should take 10–40 sec).

        (v) Rinse the basket with copious amounts of water to remove the bleach.

        (vi) Remove the water from the bottom with a paper towel.

    ▲ **CRITICAL STEP** do not over-bleach the embryos to ensure their viability and normal development.

    (B) Dechorionation with needle

        (i) Prepare a microscope slide with double-sided tape on one side of it.

(ii) Transfer the embryos into a basket with a paintbrush.

(iii) (iii) Remove the oil from the bottom with a paper towel.

(iv) Rinse the embryos with a few ml of water.

(v) Transfer embryos to the sticky tape on the slide prepared in step 5 Option B(i).

(vi) Use a needle or thumbtack to gently tear the chorion open.

(vii) Use a paintbrush to gently remove the embryo from chorion. (see video step 7 in [23] for details).

▲ CRITICAL STEP after dechorionation, the embryos are more fragile, therefore they should only be gently manipulated. Minimize the time they spend in the air without water.

6| Gently transfer the embryos onto an agarose plate (see Reagent Setup). Once placed on this plate, the water content of the agarose gel prevents them from drying.

7| Align and orient the embryo dorsal side up in the center of the agarose plate.

▲ CRITICAL STEP from step 6 to step 8, the embryos have to be kept as clean as possible: any piece of chorion, dust, or agarose sticking to their surface can have a large negative impact on the imaging quality.

? TROUBLESHOOTING

8| Cut the central piece of agar and transfer it under a dissecting scope.

9| Gently stick the embryos to a coverslip coated with glue (see Equipment Setup) by bringing the coverslip glue-side down towards the embryos until they just touch the coverslip. Turn over the coverslip and add a water droplet on top of them.

▲ CRITICAL STEP be careful not to crush the embryos with the coverslip.

4D-Imaging ● TIMING 3h per imaging acquisition

10| Using an inverted Zeiss LSM microscope, add a water droplet onto the long working distance water objective. Place the coverslip (from step 9) under the microscope with the embryos facing the objective. Bring the embryos into focus using brightfield transmitted illumination to avoid any bleaching of GFP.

11| Adjust the femtosecond laser to 940nm wavelength. Adjust the mean power to a level no higher than ~20mW at the objective focus (use a powermeter to check it).

12| Choose a well-oriented embryo at early stage 6[10] with the ventral furrow facing the objective, in the middle of the field of view. Adjust the position and field of the acquisition. Use a 200μm × 200 μm square field in the center of the embryo (Fig. 3a and Supplemental Movie 2). Select the appropriate spatial and temporal sampling as discussed in the introduction: typically 0.5 μm per pixel in x and y, and 1μm in z; 45–50 sec of time between each z-stack including 10 sec of resting time. Adjust the number of z-slices to image such that data is acquired from the most ventral ectoderm cells to the expected position of the most dorsal mesoderm cells when the ventral furrow is fully formed (typically 80 μm z-stack).

13| Adjust the photomultiplier tube (PMT) gain to avoid any saturation of the fluorescent signal from the mesoderm cells at every z-position. Saturation occurs when the

signal detected causes the pixel to reach its maximum value (255 for a 8bit-image). There will be some saturation in the fluorescent signal from the ectoderm.

14| Run the time-lapse acquisition for 3 h at 25 °C. Monitor the temperature during acquisition: it is critical as the speed of development is highly sensitive to the temperature (development proceeds at rate approximately twice as fast at 25 °C compared to 18 °C).

■ PAUSE POINT Store the acquisition data until use. The rest of the protocol can be paused at anytime.

? TROUBLESHOOTING

15| Repeat steps 1–15 several times in order to obtain a good imaging dataset (i.e., no phototoxicity, good orientation, good signal-to-noise ratio, correct time and spatial window, sufficient number of cells staying within the field of view).

3D-Cell Tracking ● TIMING weeks

16| Load and visualize the imaging datasets in 3D using Imaris. Select a good data set (see step 15) and crop it in time and space to focus on the useful time and spatial window. Verify the spatial calibration (size of voxels in μm/pixel) corresponds to your microscope calibration. Save the file as EmbryoSequence.ims

▲ CRITICAL STEP In order to perform the 3D-cell tracking efficiently and reduce the time spent to do it, extensive knowledge of Imaris software is recommended. The user is invited to follow Bitplane user training sessions or to contact Bitplane customer service for further information.

? TROUBLESHOOTING

17| Segment nuclear position using Imaris spot detection: adjust the size to 4–5 μm.

? TROUBLESHOOTING

18| Track the cell movements using Imaris spot tracking. Use "autoregressive motion" option with gap size set to 2 as the scripts provided to analyze the data are not designed for a larger gap.

19| Sort and manually correct the tracks using the Tracking Editor, so that each track is complete from the beginning to the end of the sequence. However, keep in mind that the scripts provided to analyze the data handle only one-branch tracks, meaning that each track has a maximum of one spot per time point (see annotations in Matlab scripts for details, **Supplementary Data 1**). This is a concern since after a cell division only one daughter will acquire the initial track sequence. Manual correction is required. First, detect the cell divisions manually. Subsequently, duplicate each track before a cell division so that each daughter cell has its own track from beginning to end.

20| Complete the tracking data using manual spot detection and tracking. Save the scene file as EmbryoSequence.imx

21| Perform steps 17–20 successively for mesoderm cells, ectoderm cells and a few cells (typically 8) from the midline. Use Imaris functions to select the tracks from the corresponding subpopulation of cells. The midline cells can be visually discerned and tracked manually (**Supplemental Movie 3**). Because the ectoderm is only used as a reference, the tracks from the ectoderm do not need to be complete (ie. not all tracks have to go from beginning to end and some cells can be missing) for the subsequent analysis: typically 50% of cells tracked representing the ectoderm

movement is sufficient. No need to identify the daughter cells after division in this case.

? TROUBLESHOOTING

22| Export the tracking data using ImarisXT Object Manager into 3 different files: Mesoderm.mat, Ectoderm.mat and Midline.mat

Tracking Data Registration ● TIMING 1h

23| Place the tracking data files (Mesoderm.mat, Ectoderm.mat and Midline.mat) in the same folder as the customized Matlab scripts (**Supplementary Data 1** and Table 2). One can start the procedure at this step using the sample tracking data files provided in the supplementary section of this protocol (**Supplementary Data 2**).

24| Convert Imaris tracking files into x, y, z, t matrices using Imaris2xyzt.m Matlab script. This script outputs: $x(i,j)$, $y(i,j)$, $z(i,j)$, and $t(j)$, with i and j the cell number and the time point, respectively. x, y are the image plane coordinates, z the axial direction of imaging and t the time. Enter the $t_{sequence}$, the time calibration (time delay between z-stacks). This script checks errors in the tracking dataset: if required, correct the tracking in Imaris and recheck for errors (see script annotations for details). Run the script for each Imaris tracking file (Mesoderm.mat, Ectoderm.mat and Midline.mat). Output: Midlinexyzt.mat, Mesodermxyzt.mat and Ectodermxyzt.mat.

25| Fit a cylinder on the 3D distribution of ectoderm cell positions (Fig. 4) using the EctodermCylinderFit.m Matlab script.

26| Synchronize the sequences based on the onset of GBE (Fig. 5d) using the TimeSynchronization.m Matlab script.

27| Perform the final registration (Fig. 5a–c) of the tracking data using Registration.m Matlab script. The registered mesoderm cell tracking data (xReg, yReg, zReg, and tReg matrices) are saved into the MesodermReg.mat file.

Tracking Data Analysis ● TIMING 1h

28| A number of different analyses can be performed after tracking data registration[1]. For example, to decompose the cell trajectories into their cylindrical components use Option A below. To perform a statistical analysis of the mesoderm cell migration and quantify its collective nature, use option B.

  (A) **Display the tracking data** using MovementDecomp.m Matlab script (Fig. 6).

   (i) Run MovementDecomp.m Matlab script and follow the instructions. The mesoderm cell 3D trajectories are decomposed along each cylindrical coordinate ($r(t)$, $\theta(t)$, and $z(t)$) as displayed in Fig. 6.

  (B) **Analyze the mesoderm cell spreading** using SpreadingAnalysis.m (Fig. 7).

   (i) Run SpreadingAnalysis.m and follow the instructions. It displays the spreading analysis of mesoderm cells: spatial organization as in Fig. 7c and $\theta_{end}(\theta_{start})$ graph with the the statistical analysis results as in Fig. 7d.

TIMING

Steps 1–9, **Embryo Preparation**: 4 h per set of embryos for imaging.

Steps 10–15, **4D-Imaging**: 3 h per imaging acquisition. Repeat steps 1–15 **s**everal times to obtain 3–4 correct imaging datasets: ~ 1 week.

Steps 16–22, **3D-Cell Tracking**: several weeks per imaging dataset depending on the quality of the dataset and on the efficiency of the user to perform the tracking correction with Imaris.

Steps-23–27, **Tracking Data Registration**: 1 h maximum per dataset.

Step 28 **Tracking Data Analysis**: 1 h maximum per dataset.

TROUBLESHOOTING

Troubleshooting advice is provided in Table 3.

ANTICIPATED RESULTS

The imaging and the 3D cell-tracking (steps 1–22) should result in the visualization of mesoderm and ectoderm cell distributions (Fig. 3b and Supplementary Movie 1) and the spreading movement of mesoderm cells during gastrulation (Fig. 3c). The visualization of a 4D imaging dataset is available within published work[1].

The results of tracking data registration (steps 23–27) obtained with the sample tracking data provided in supplemental section of this protocol (**Supplementary Data 2**) are displayed in Fig. 4–5. First, the ectoderm cell positions are fitted onto a cylinder using EctodermCylinderFit.m script (step 25), which displays the distribution of a selected number of ectoderm cells on an estimated cylinder as in Fig. 4c. The time synchronization using TimeSynchronization.m script (step 26) shows the movement of the mesoderm cells toward the posterior direction and estimates the time point at which the onset of movement occurs (Fig. 5d). The Registration.m script (step 27) displays the angular movements of mesoderm cells before and after angular drift correction, as in Fig. 5a–c.

After the tracking data registration, the decomposition of mesoderm cell movements into their cylindrical components $r(t)$, $\theta(t)$, and $z(t)$ using MovementDecomp.m script (step 28A) should result in the three graphs of Fig. 6. Each of these graphs corresponds to a specific morphogenetic event: (i) $r(t)$ shows the furrow collapse with the cells moving toward the periphery of the embryo (Fig. 6a); (ii) $\theta(t)$ shows the angular spreading of the mesoderm cells with movements toward the left and right directions (Fig. 6b); (iii) $z(t)$ shows the movement of GBE with a concerted movement toward the posterior direction (Fig. 6c).

The analysis of mesoderm spreading using SpreadingAnalysis.m (step 28A) should display the two graphs of Fig. 7c and Fig. 7d. The first graph displays $\theta(t)$ for each cell with a color coding for the angular position at the onset of furrow collapse. It shows that the angular distribution of the mesoderm cells is maintained over the two hours of mesoderm spreading (Fig. 7c). The $\theta_{end}(\theta_{start})$ graph (Fig. 7d), is used to investigate the collective migration of mesoderm cells during their spreading. The position of each cell in this graph corresponds to a specific movement behavior detailed in (Fig. 7a–b). When $\theta_{end}/\theta_{start}>1$ (white areas in the graphs), the cells are spreading normally. If $0<\theta_{end}/\theta_{start}<1$ (light gray areas in the graphs), the cells are not spreading and move in the opposite direction, toward the midline. If $\theta_{end}/\theta_{start}<0$ (dark gray areas in the graphs), the cells are not spreading, cross the midline and move to the opposite end of the embryo. In wild-type embryos, the cells position in the $\theta_{end}(\theta_{start})$ graph are mainly distributed in the white area (Fig. 7d). In addition, they tend to be aligned along a specific line: a linear regression gives an estimation of the slope of this line (A) and of the correlation coefficient (R) (Fig. 7d). As previously reported[1], A and R values should be close to 2 and 1, respectively. This statistical analysis provides a quantitative tool for investigating

the collective behavior exhibited by mesoderm cells during their spreading. The behavior is quantitatively defined as the spreading strength A, which corresponds to the typical value of $\theta_{end}/\theta_{start}$. The collective nature of the process is quantified by R: a value close to 1 demonstrates the spreading behavior A=$\theta_{end}/\theta_{start}$ is shared by the entire cell population, as in wild-type embryos; a lower value means the cell spreading is disrupted, as in mutants. This quantitative analysis has been used to demonstrate (i) the reproducibility of the collective behavior in wild-type embryos and (ii) the disruption of the process and the identification of different cell populations in a mutant embryo[1].

The procedure described in this paper details every experimental step from the preparation of embryos for imaging to the quantitative analysis of mesoderm cell spreading. In addition to this analysis (step 28), the cell movements can be analyzed in whatever manner a user finds interesting by developing their own customized Matlab scripts to analyze the registered data (step 27).

Box 1. How to characterize the optical properties of a biological sample in 2PEF microscopy.

In most biological tissues, light scattering is the main physical process limiting the depth of imaging. In 2PEF microscopy, it can be characterized experimentally by measuring l_s^{ex}, the scattering mean free path of the excitation light. This length provides an estimate of the maximum depth of imaging and allows for comparison of the imaging conditions between different biological samples. If light absorption and optical aberrations can be neglected, and assuming the fluorescence collection efficiency is constant within the depths of imaging[15], the detected 2PEF signal F from a homogeneous fluorophore distribution is expected to scale as[24]:

$$F(z) \propto \left[P_0 \cdot \exp\left(-\frac{z}{l_s^{ex}}\right) \right]^2$$

[1]

where z and P_0 are the imaging depth and the average incident laser power at the tissue surface, respectively. Hence, l_s^{ex} is experimentally estimated by acquiring a z-stack of images through the sample with a given incident power, by measuring the average 2PEF signal $\langle F(z) \rangle$ in a homogenous area at each z-position and the background signal $F_{background}$, and by plotting $G(z) = \frac{1}{2}\ln\left[\langle F(z) \rangle - F_{Background} \right]$. A linear regression on G(z) provides an estimate of the slope as $-1/l_s^{ex}$ (Fig. 2c). We measured l_s^{ex} at 940 nm in the mesoderm and ectoderm tissues in wild-type and *klar* embryos at stage 8 as 56 μm and 76 μm, respectively (Fig. 2d). The estimation of l_s^{ex} displays the typical 2PEF signal decay based on equation [1] (Fig. 2e). This graph shows that at 80μm in depth, the signal in wild-type embryos at stage 8 is low (blue line) and twice as much signal can be expected in a *klar* mutant at the same stage (red line). As a comparison, we provide l_s^{ex} measurements and signal decay in stage 5 *Drosophila* embryos and in zebrafish embryos from previous reports[11, 17] (Fig. 2d–e). It demonstrates that the optical properties of embryonic tissues and the subsequent limitation of imaging depth is highly stage- and species-dependant.

Supplementary Material

Refer to Web version on PubMed Central for supplementary material.

Acknowledgments

REFERENCES

1. McMahon A, Supatto W, Fraser SE, Stathopoulos A. Dynamic Analyses of Drosophila Gastrulation Provide Insights into Collective Cell Migration. Science 2008;322:1546–1550. [PubMed: 19056986]

2. Keller PJ, Schmidt AD, Wittbrodt J, Stelzer EHK. Reconstruction of Zebrafish Early Embryonic Development by Scanned Light Sheet Microscopy. Science 2008;322:1065–1069. [PubMed: 18845710]

3. Leptin M, Grunewald B. Cell shape changes during gastrulation in *Drosophila*. Development 1990;110:73–84. [PubMed: 2081472]

4. Kam Z, Minden JS, Agard DA, Sedat JW, Leptin M. Drosophila gastrulation: analysis of cell shape changes in living embryos by three-dimensional fluorescence microscopy. Development 1991;112:365–370. [PubMed: 1794308]

5. Irvine KD, Wieschaus E. Cell intercalation during *Drosophila* germband extension and its regulation by pair-rule segmentation genes. Development 1994;120:827–841. [PubMed: 7600960]

6. Bertet C, Sulak L, Lecuit T. Myosin-dependent junction remodelling controls planar cell intercalation and axis elongation. Nature 2004;429:667–671. [PubMed: 15190355]

7. Smallhorn M, Murray MJ, Saint R. The epithelial-mesenchymal transition of the Drosophila mesoderm requires the Rho GTP exchange factor Pebble. Development 2004;131:2641–2651. [PubMed: 15128661]

8. Debarre D, et al. Imaging lipid bodies in cells and tissues using third-harmonic generation microscopy. Nat. Methods 2006;3:47–53. [PubMed: 16369553]

9. Welte MA, Gross SP, Postner M, Block SM, Wieschaus EF. Developmental regulation of vesicle transport in Drosophila embryos: Forces and kinetics. Cell 1998;92:547–557. [PubMed: 9491895]

10. Hartenstein, V. Atlas of Drosopbila Development. In: Bate, M.; Martinez Arias, A., editors. The Development of Drosophila melanogaster. Cold Spring Harbor Laboratory Press; New York, USA: 1993. p. 36-52.

11. Supatto W, Fraser SE, Vermot J. An all-optical approach for probing microscopic flows in living embryos. Biophys. J 2008;95:L29–L31. [PubMed: 18556762]

12. Supatto W, et al. In vivo modulation of morphogenetic movements in Drosophila embryos with femtosecond laser pulses. Proc. Natl. Acad. Sci. U. S. A 2005;102:1047–1052. [PubMed: 15657140]

13. Hopt A, Neher E. Highly nonlinear photodamage in two-photon fluorescence microscopy. Biophys. J 2001;80:2029–2036. [PubMed: 11259316]

14. Ji N, Magee JC, Betzig E. High-speed, low-photodamage nonlinear imaging using passive pulse splitters. Nat. Methods 2008;5:197–202. [PubMed: 18204458]

15. Beaurepaire E, Mertz J. Epifluorescence collection in two-photon microscopy. Appl. Optics 2002;41:5376–5382.

16. Vermot J, Fraser SE, Liebling M. Fast fluorescence microscopy for imaging the dynamics of embryonic development. HFSP J 2008;2:143–155. [PubMed: 19404468]

17. Debarre D, et al. Velocimetric third-harmonic generation microscopy: micrometer-scale quantification of morphogenetic movements in unstained embryos. Opt. Lett 2004;29:2881–2883. [PubMed: 15645811]

18. Zamir EA, Czirok A, Cui C, Little CD, Rongish BJ. Mesodermal cell displacements during avian gastrulation are due to both individual cell-autonomous and convective tissue movements. Proc. Natl. Acad. Sci. U. S. A 2006;103:19806–19811. [PubMed: 17179040]

19. Liebling M, Forouhar AS, Gharib M, Fraser SE, Dickinson ME. Four-dimensional cardiac imaging in living embryos via postacquisition synchronization of nongated slice sequences. J. Biomed. Opt 2005;10

20. Tyszka JM, Ewald AJ, Wallingford JB, Fraser SE. New tools for visualization and analysis of morphogenesis in spherical embryos. Dev. Dyn 2005;234:974–983. [PubMed: 16193511]

21. Guan, JL. Cell migration: developmental methods and protocols. Humana Press; Totowa, NJ: 2005.

22. Greenspan, RJ. Fly pushing: the theory and practice of Drosophila genetics. Cold Spring Harbor Laboratory Press; Cold Spring Harbor, NY: 2004. p. 17-21.

23. Reed B, McMillan S, Chaudhary R. The Preparation of Drosophila Embryos for Live-Imaging Using the Hanging Drop Protocol. JoVE 2009;25

24. Oheim M, Beaurepaire E, Chaigneau E, Mertz J, Charpak S. Two-photon microscopy in brain tissue: parameters influencing the imaging depth. J. Neurosci. Methods 2001;111:29–37. [PubMed: 11574117]
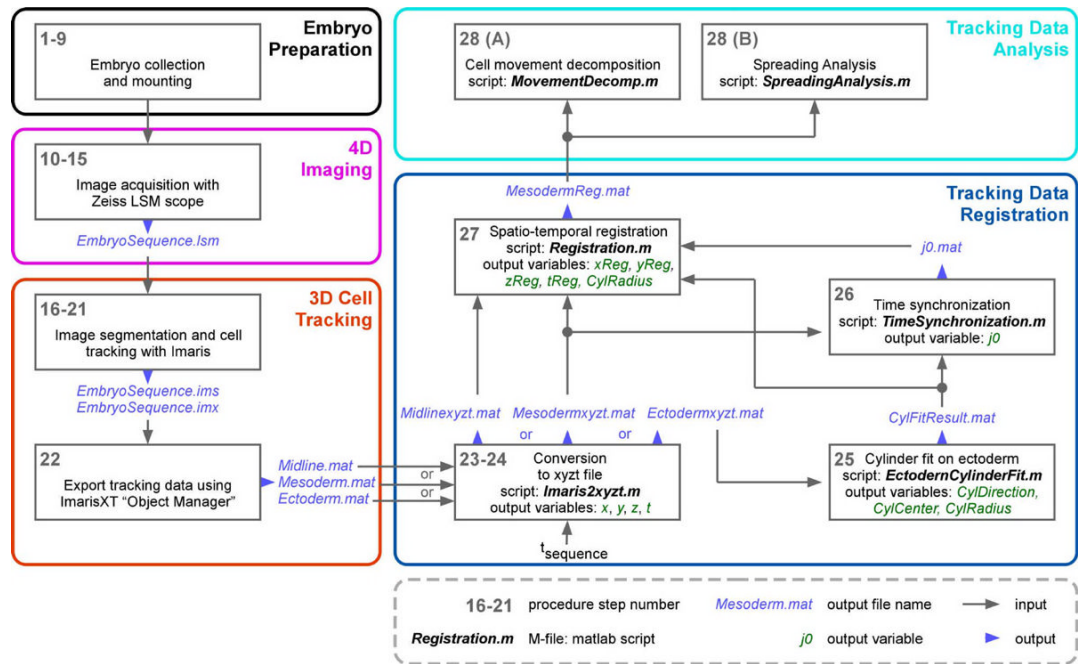
Figure 1.
The experimental work-flow describes the five main parts of the protocol: embryo preparation (black box), 4D-imaging (magenta box), 3D cell tracking (red box), tracking data registration (blue box) and tracking data analysis (cyan box).
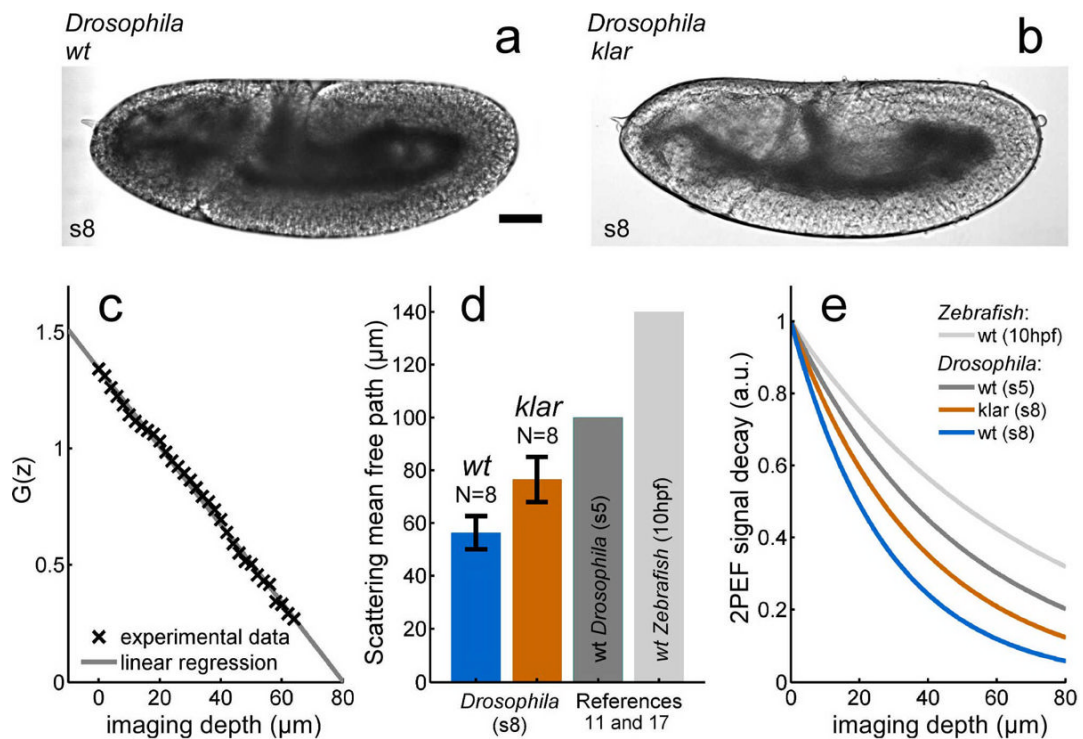
Figure 2.
Optical properties of mesoderm in early *Drosophila* and zebrafish embryos. Using brightfield microscopy, wild-type *Drosophila* embryos (a) at stage 8 (s8) appear darker than *klarsicht* mutants (b), which is due to the different light scattering properties of the cells. The experimental quantification of these optical properties is performed as explained in **Box 1**. Each fluorescent imaging dataset is analyzed by plotting G(z) (see **Box 1** for its definition) and fitting the experimental data using a linear regression (c). This analysis allows estimation of the scattering mean free path l_s^{ex} of the excitation light from embryonic tissues at different stages or from different species (d). The graph (d) shows that *klarsicht Drosophila* embryos (red) exhibit $l_s^{ex} \sim 76$ μm, which is 20 μm larger than wild-type embryos at the same stage (blue). The error bars represent the standard deviation of the l_s^{ex} estimations for N=8 embryos. Previous studies show that similar measurements performed in *Drosophila* blastoderm cells at stage 5 (s5) and in Zebrafish mesoderm cells at bud stage (10hpf, hours post fertilization) result in l_s^{ex} two and three times larger, respectively[11, 17] (dark and light gray in d, respectively). These measures are used to plot the typical 2PEF signal decay in depth (e) as explained in **Box 1**. This graph displays the loss of fluorescence signal when imaging deeper inside an embryonic tissue and permits comparison of the expected signal loss observed in tissues with different optical properties. It shows that the difference in optical properties between wild-type *Drosophila* (blue curve) and *klarsicht* (red curve) s8 embryos is significant, and results in the ability to obtain twice the fluorescent signal at 80 μm within *klarsicht* embryos. 80 μm is the position of the deepest mesoderm cells in this embryo. It also shows that the signal is 3 times higher in wild-type *Drosophila* at s5, and 5 times higher in zebrafish embryos under similar imaging conditions (dark and light gray curves at 80 μm, respectively). Scale bar in (a) indicates 50μm. *wt*: wild-type
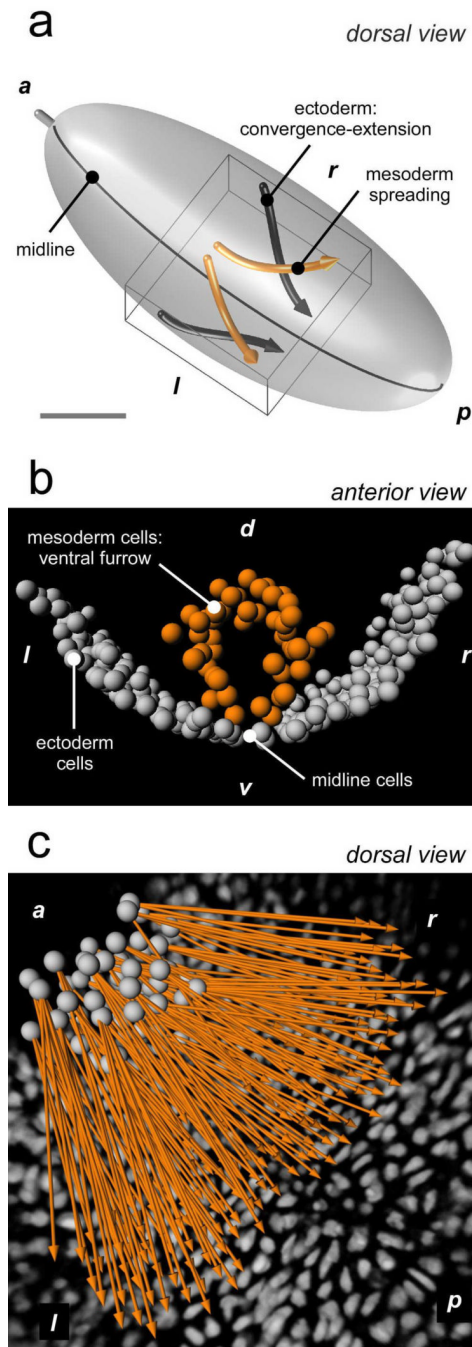
Figure 3.
Typical image processing results with Imaris. The 3D-schematic representation of the embryo (a) shows the position of the imaging field of view (boxed region), the movements of ectoderm convergence-extension (black arrows) and of mesoderm spreading (orange arrows). The 3D-segmentation of the cell nuclei on the ventral side of the embryo at the onset of mesoderm spreading (b) shows the cylindrical shape of the ectoderm layer (gray spheres) and the furrow formed by the mesoderm cells (orange spots). The 3D-tracking of mesoderm cells (c) (gray spots in c) and their overall displacement (orange arrows) show the combination of movement toward the posterior direction due to germband extension (GBE) and the angular spreading in the left and right directions. 3D view. Scale: the scale bar in (a) indicates 50 μm; the spots in

(b–c) are 5 µm diameter. Gray in (c): imaging data of ectoderm cells. *a*: anterior, *p*: posterior, *l*: left, *r*:right, *d*: dorsal, *v*: ventral. (Figure 3B is reproduced with permission from AAAS[1]).
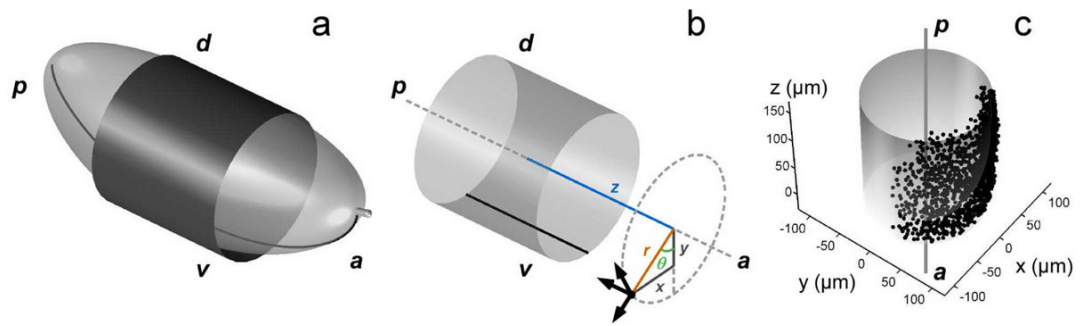
Figure 4.
Cylinder fit on the spatial distribution of ectoderm cell positions obtained with EctodermCylinderFit.m script (step 25). The part of the embryo imaged has a cylindrical shape (a) with its main direction aligned with the anterior-posterior direction. The cylindrical coordinate system (b) is obtained after fitting a cylinder on the distribution of ectoderm cells (a and c). After the final registration (step 27), the Cartesian reference frame is rotated and the z-axis is aligned with the anterior-posterior axis of the embryo as in (c). The angular position of the midline (black line in a and b) defines the value θ=0. *a*: anterior, *p*: posterior, *d*: dorsal, *v*: ventral.
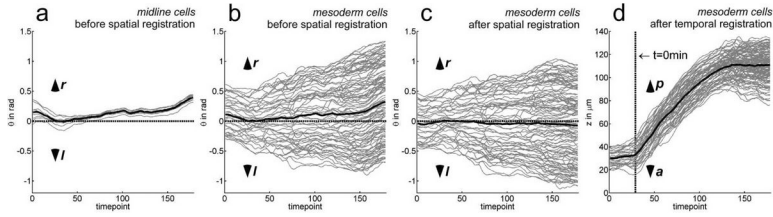
Figure 5.
Spatial and temporal registration (step 26 and 27). The Registration.m script subtracts the average angular movement of midline cells (a) from the angular movement of mesoderm cells (b) to obtain a correction of the angular drift (c). After correction, the average angular position of mesoderm cells (black line in b–c) remains close to 0 during the entire spreading process, showing the symmetrical nature of the spreading. The TimeSynchronization.m script identifies the onset of germband extension (GBE, at t=0 min) and displays the mesoderm cell movement toward the posterior direction (d). The gray lines represent the trajectories of midline cells (a) or mesoderm cells (b–d). The black line is the average trajectory of the cell population. The dashed gray lines in (a–c) show θ=0 rad position. The dashed gray lines (d) shows t=0 min position. The timepoints (horizontal axis of the graphs) represent the image number within the sequence; after temporal synchronization these timepoints are converted into minutes. *a*: anterior, *p*: posterior, *l*: left, *r*:right, *d*: dorsal, *v*: ventral. rad: radians.
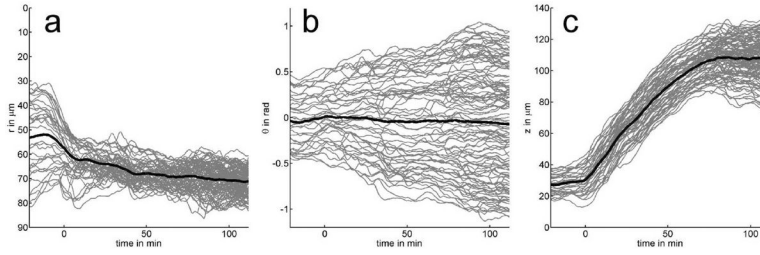
Figure 6.
Decomposition of mesoderm cell movements into their cylindrical components using MovementDecomp.m (step 28A). This script decomposes the registered trajectories of mesoderm cells into their cylindrical components (r, θ, and z, for radial, angular and longitudinal components, respectively) and plots the three graphs r(t), θ(t), and z(t) as displayed in this figure ((a), (b), and (c), respectively). The gray lines represent the trajectories of mesoderm cells along each cylindrical direction. The black line is the average trajectory of the cell population. In the radial direction (a), r=0 corresponds to the center of the embryo and mesoderm cells moving toward positive values of r are moving closer to the ectoderm layer, at the periphery of the embryo. The graph r(t) shows the furrow collapse with the cells moving toward the ectoderm (a). In the angular direction (b), θ=0 corresponds to the position of the ectoderm midline and the cells moving toward positive or negative values of θ are moving toward the right or left side of the embryo, respectively. The graph θ(t) shows the angular spreading of the mesoderm cells with movements toward the left and right directions (b). In the longitudinal direction (c), z=0 is arbitrarily chosen, and the cells moving toward positive or negative values of z are moving toward the posterior or anterior side of the embryo, respectively. The graph z(t) shows the movement of GBE with a concerted movement of mesoderm cells toward the posterior direction (c). rad: radians
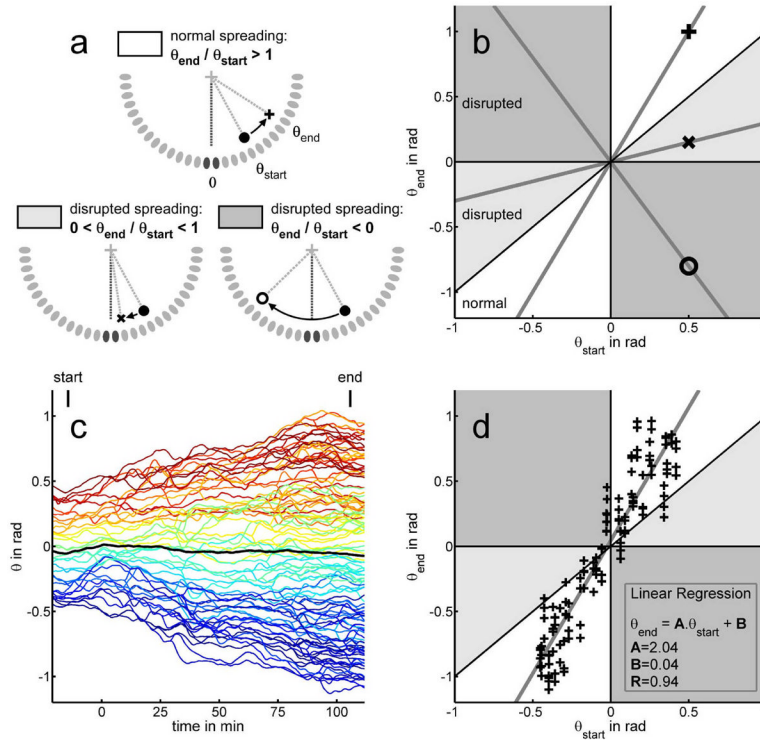
Figure 7.
Analysis of mesoderm cell spreading using SpreadingAnalysis.m (step 28B). (a) Three specific cell movements are identified. First, a cell moving from θ_{start} to θ_{end} (angular positions at the onset and at the end of the process, respectively) with $\theta_{end} / \theta_{start} > 1$ corresponds to a normal spreading behavior (white area). In this case, the cell (+ sign) is moving on top of the ectoderm layer (gray ovals), further away from the midline position (black ovals, $\theta=0$ position). A disrupted spreading (light gray area) with cells moving toward the midline (x sign) corresponds to $0 < \theta_{end} / \theta_{start} < 1$. Finally, the most disrupted behavior (dark gray area) corresponds to a cell crossing the midline (o sign) and moving on the opposite side of the embryo with $\theta_{end} / \theta_{start} < 0$. These three behaviors correspond to three different areas of the $\theta_{end}(\theta_{start})$ graph (b): white, light gray and dark gray, respectively. The movement of each cell is represented by a point on this graph and the slopes of the gray lines is the $\theta_{end} / \theta_{start}$ in each case (normal spreading, + sign and disrupted movements, x and o signs). This representation is used by the script to analyze the spatial organization of the cell movements in the angular direction. It first displays $\theta(t)$ for each cell with a color coding for the angular position at the onset of the furrow collapse (c) and the $\theta_{end}(\theta_{start})$ graph (d). The experimental data obtained from a wild-type embryo (+ signs in d) are mainly located in the white area of the graph, corresponding to a normal spreading. This distribution is analyzed using a linear regression as described in Anticipated Results. The result of the regression is dispayed on the graph (gray line and values A, B and R, see Anticipated Results for details). rad: radians. (Figure 7d is modified with permission from AAAS1).

Table 1

Experimental recommendations to investigate the collective migration of large cell population in a live embryo using quantitative imaging and analysis. The experimental workflow (see Fig. 1) is not specific to the study of *Drosophila* gastrulation. The table summarizes several general experimental recommendations for any model system. The specific experimental choices made to study *Drosophila* mesoderm spreading are indicated and discussed in the text

Workflow step		General recommendations	*Drosophila* mesoderm spreading
Embryo Preparation	*Fluorescent labeling*	Strong and ubiquitous labeling of nuclei (histone labeling better than nuclear localization sequence to follow cell division)	H2A-GFP line
	Stabilization	Avoid motion artifacts by holding the embryo in place during the acquisition time.	Embryos are glued to a coverslip
	Mounting setup	Embryo mounting optically adapted for efficient microscopy	Embryos are imaged directly through water without coverslip
4D imaging	*Microscope*	Adapted technique of microscopy depends on the sample/process to image	2PEF microscopy Objective: 40× / 1.1NA / water immersion / large working distance For scattering tissue imaging: improved photon collection and *klarsicht* line with improved optical properties.
	Field of view Spatial / temporal resolution	Compromised between proper image processing and low phototoxicity. Spatial sampling critical for proper nuclear segmentation. Temporal sampling critical for proper tracking. Field of view adapted to the dynamic process.	200μm × 200μm × 200μm field of view 45 s time sampling 0.5μm × 0.5μm × 1μm spatial sampling
	Excitation wavelength	Compromised between efficient fluorophore excitation, low phototoxicity and endogenous signal excitation.	Excitation at 940nm Good GFP excitation, low phototoxicity and low background
	Phototoxicity	Acquisition parameters (field of view, spatial/temporal sampling, laser power, resting time, wavelength) adjusted to limit phototoxicity.	Mean power < 30mW 10 s resting time between z-stack acquisitions
3D cell tracking	*3D-segmentation*	Spatial sampling and signal to noise ratio critical for proper nuclear segmentation. Manual correction can be useful.	Signal level critical: the use of *klarsicht* mutant and improved photon collection facilitate nuclear segmentation. Use of Imaris.
	3D-tracking	Temporal sampling critical for proper tracking. Motion artifacts (embryo rolling, stage or sample drift, etc.) can drastically deteriorate tracking efficiency. If so, spatial registration is required before 3D-cell tracking step. Manual correction can be useful Export of tracking results for further analysis.	*Drosophila* develops fast: 45 s of temporal sampling is critical. Use of Imaris and data export into Matlab.
Data Registration	*Spatial registration: Motion artifact correction*	Correction of motion artifacts (embryo rolling, stage or	Segmented-based registration Angular drift correction using the tracking of

	Workflow step	General recommendations	*Drosophila* mesoderm spreading
		sample drift, etc.) can be done before or after cell tracking.	ectoderm midline cells. Matlab Processing.
	Spatial registration: coordinate system	Spatial coordinate system adapted to biological structure (body plan, polarity,etc.). Adjustment of a reference frame to the dataset.	Cylindrical coordinate system Fit of a cylinder on the ectoderm cell layer. Matlab processing.
	Temporal registration: synchronization	Synchronization of image sequences based on a biological event not disrupted in the mutant (onset of movement, etc.).	Synchronization using the onset of GBE. Matlab Processing.
Tracking Data Analysis	*Movement decomposition*	Complex 3D cell motions: decomposition along each spatial direction using a coordinate system meaningful for the biology. Color-coding trajectories can be useful.	Morphogenetic movements decomposed in the cylindrical coordinate system. Color coding for angular position reveals spatial organization of cell migration. Matlab Processing.
	Statistical analysis of collective motion	Statistical analysis depends on the nature/geometry of the collective process.	$\theta_{end}(\theta_{start})$ graph exhibits collective migration of mesoderm cells. Collective nature quantified by the correlation coefficient obtained from a linear regression. Matlab Processing.

Table 2

Description of the customized Matlab scripts contained in Supplementary Data 1.

Matlab script name	Description
Imaris2xyzt.m	Converts the tracking data exported by ImarisXT Object Manager into x, y, z, t matrices. x(i,j), y(i,j), z(i,j), and t(j) are the spatial cartesian coordinates in μm and the time in minute of each cell i at each time point j. i and j are integers. In case the tracking data appear noisy (i.e., trajectories with small movements at high frequency), this script can smooth them in time by using a 5-point Loess quadratic fit applied to each spatial component. Requires Imaris tracking files (Mesoderm.mat, Ectoderm.mat or Midline.mat) and stores the results in Mesodermxyzt.mat and Ectodermxyzt.mat or Midlinexyzt.mat files, respectively.
EctodermCylinderFit.m	Fits a cylinder on the distribution of ectoderm cell positions (Fig. 4c). Estimates the direction (CylDirection), the center (CylCenter) and the radius (CylRadius) of the cylinder. Requires Ectodermxyzt.mat and stores the result into the file CylFitResult.mat.
TimeSynchronization.m	Estimates j0, the time point for which t=0 min as the onset of GBE by checking the mesoderm cell movements toward the posterior direction (Fig. 5d). Requires Mesodermxyzt.mat and CylFitResult.mat and stores j0 in the j0.mat file.
Registration.m	Spatial and temporal registration of the tracking data. Registers the time matrix t by using the j0 value. Rotates in 3D the Cartesian reference frame using the cylinder fit result so that the z-axis is aligned with the embryo anterior posterior direction (main axis of the cylinder). In this frame, the new Cartesian components x, y, and z can be directly converted into the cylindrical components r, θ, and z using the cart2cyl.m function from geom3d toolbox. An additional rotation of the frame along the anterior-posterior axis creates the mesoderm cell angular positions θ in the [-π/2 π/2] range using cart2cyl0.m function. Corrects the angular drift of mesoderm cells using the midline tracking data (Fig. 5a–c). Requires Mesodermxyzt.mat, Midlinexyzt.mat, CylFitResult.mat and j0.mat. Stores the registered mesoderm cell tracking data (xReg, yReg, zReg, and tReg matrices) into the MesodermReg.mat file.
MovementDecomp.m	Loads the MesodermReg.mat file and converts the Cartesian coordinates into the Cylindrical coordinates. Plots the time variation of each component (r(t), θ(t), and z(t)) for each cell into three graphs as displayed in Fig. 6. Requires MesodermReg.mat file.
SpreadingAnalysis.m	Loads the MesodermReg.mat file and converts the Cartesian coordinates into the Cylindrical coordinates. Displays θ(t) for each cell with a color coding for the angular position at the onset of the furrow collapse, as in Fig. 7c. Identifies this timepoint (jstart) as the time when the furrow has a cylindrical shape. Displays the angular position at the end of the spreading θ_{end} (defined as 120 minutes after jstart) depending on the angular position at the onset θ_{start} (at jstart) for each cell. Performs a linear regression on the distribution of the points in this graph and the result is displayed on it as in Fig. 7d. Requires MesodermReg.mat file.
Browse.m	Browse function.
cart2cyl0.m	Converts cartesian to cylindrical coordinates. This function is similar to cart2cyl.m from the geom3d toolbox but return θ in [−π], instead of in [0 2θ].

Table 3

TROUBLESHOOTING

Step	Problem	Possible reason	Solution
7 and 16	Mis-orientation	Embryo not well-oriented	Orient the embryos carefully.
		Embryo rolling inside the vitelline membrane	Manipulate the embryo more gently and for the shortest amount of time possible.
14	Signal vanishes during acquisition	Water evaporation	Add more water between the coverslip and the objective
16	Toxicity	Embryo does not develop	Normal: 80% survival rate in wt embryos. Over-bleaching: try using the Sigma bleach for more control of the hypochlorite concentration, or bleach for a shorter amount of time. Make sure to rinse embryos thoroughly after bleaching. Manipulation: dechorionated embryos are fragile and can only survive for a short period of time without water or oil and must be manipulated gently (steps 7– 10).
		Embryo develops but movement or cell division is disrupted	Reduce laser power Increase rest time between stacks
16	Whole embryo movement during the acquisition	Embryo detached from the glue	Use more glue on the coverslip
17	False positive segmentation	Noisy signal	Remove any source of ambient light during acquisition (e.g., room lights, computer LEDs).
		Spot size not correct	Adjust spot size (increasing size usually decreases noise).
21	Erroneous cell tracking	Time sampling too low	Increase the time resolution or decrease the temperature to slow down development.
21	Imaris slow	Too many spots/tracks	Partition your dataset: cut the datasets into several time windows and perform the analysis on each part
			Remove unnecessary spots/tracks from the scene Use a faster computer